Observer-Based Wheelbase Preview Control of Active Vehicle Suspensions

Hyoun-Surk Roh* and Youngjin Park*

(*Received September 4, 1997*)

Optimal observer-based wheelbase preview regulator problem is investigated for active vehicle suspension systems. It is shown that the problem reduces to the classical linear quadratic Gaussian problem, whose solution is well defined, by augmenting dynamics of system and road inputs. The resulting optimal controller is in the form of augmented state feedback controller and this augmented state is estimated by Kalman-Bucy filter using dynamics of the augmented system. Numerical examples of a half car model are given to verify the performance improvement achievable with the proposed controller.

Key Words: Wheelbase Preview, Observer, Active Suspnsion

Nomenclature

A	: Continuous-time system matrix in state equation
a, (b)	: Distance between center of mass of main vehicle body and front (rear) suspension
B	: Continuous-time input distribution matrix in state equation
C	: Continuous-time output matrix in output equation
D	: Continuous-time input distribution matrix in output equation
E	: Continuous-time disturbance distribution matrix in state equation
F	: Discrete-time equivalent of E
G	: Discrete-time equivalent of A
H	: Discrete-time equivalent of B
I	: Moment of inertia of main vehicle body
k_{f1}, (k_{r1})	: Stiffness connecting main vehicle body and front (rear) axle
k_{f2}, (k_{r2})	: Front (rear) tire stiffness
L	: Continuous-time disturbance distribution matrix in output equation
M	: Mass of main vehicle body
m_f, (m_f)	: Mass of front (rear) axle
v	: Vehicle speed (m/sec)
z_{0f}, (z_{0r})	: Front (rear) road displacement (m)
ω	: Circular frequency (rad/sec)

* NoViC, Korea Advanced Institute of Science and Technology

1. Introduction

It is well-known that compromise between ride comfort and handling performance has to be made to design a passive suspension of a vehicle. To overcome this problem, many researchers have proposed to use active suspensions. Unlike passive systems that can only store or dissipate energy at a constant rate, active suspensions can continuously change the energy flow to or from the system when required. Furthermore, characteristics of active suspensions can adapt to instantaneous changes in driving conditions detected by sensors. As a result, active suspensions can improve both ride comfort and handling performance to satisfactory levels.

It has been first proposed by Bender that performance of active suspension can be further improved if knowledge of the road surface in front of the actively controlled axles, *i. e.*, preview information is used in the control strategy. (Bender, 1968) With preview information, we

can, for example, prepare the vehicle for future road inputs and pass through abrupt road obstacles without severe impacts.

There are two possible ways to obtain preview information. One is to use look-ahead sensors and the other is to estimate road profiles from the responses of the front wheels under an assumption that road inputs at rear wheels are the same as those at the front wheels except for time delays. By using look-ahead sensors we can obtain preview information both for front and rear suspensions, while in the case of wheelbase preview we have preview information only for the rear suspension.

The performance of look-ahead preview is generally better than that of wheelbase preview since, for wheelbase preview, preview information is only available to control of rear suspension. However, wheelbase preview may be preferred to look-ahead preview in spite of its performance limitations in some cases. First, look-ahead sensors might recognize a heap of leaves as a serious obstacle, while a ditch filled with water might not be detected at all. Second, additional implementation of preview sensors may produce a considerable cost increase. Finally, motion of the vehicle may distort the signals of look-ahead sensors that are attached to the vehicle bodies. To cope with these disadvantages of look-ahead preview, several researchers have been interested in the development of wheelbase preview controls.

Louam *et al.* applied LQR theory to derive the optimal wheelbase preview controller of two-dimensional vehicle suspension system under the assumption that state and road information is exactly known. By simulations, they showed that performance improvement more than 25% can be achieved up to 100 km/h. (Louam, 1988) Pilbeam *et al.* also derived the optimal wheelbase preview controller while considering actuator dynamics so that the resulting controller can be realized at low cost. (Pilbeam, 1993)

In two researches given above, they used the assumption that state and preview information is available. However, we cannot expect, for practical reasons, that we will have complete information on the state variables in the vehicle suspension control. In the design of the controller, we need to consider that only incomplete information on them is available. We also need to consider possibility that the measurement signals might be contaminated by sensor noises. To realize wheelbase preview control in the vehicle suspension, we should consider the estimators that will estimate state and preview information simultaneously while minimizing the effect of sensor noises on the estimation performance.

Huisman *et al.* designed a controller and an observer independently based on the different road models without proving separation theorem. Their simulations revealed that performance of the controller and the observer would be unsatisfactory. (Huisman, 1994) Yoshimura *et al.* derived the LQG-type controller by augmenting dynamics of the system and the road inputs. (Yoshimura, 1993) In their formulation, road inputs that act as system noises are correlated with one another by time delays, which makes the resulting controller different from the conventional LQG controllers. They used a simplifying assumption that is valid only when time delays between road inputs are relatively small. Therefore, the controller cannot be said an optimal one in general cases.

In this manuscript, we will derive the optimal wheelbase preview controller for vehicle suspension system with incomplete and noisy measurements in order to investigate the possible performance improvement with wheelbase preview. It will be shown that design of the controller which will be called stochastic optimal observer-based wheelbase preview regulator problem reduces to the conventional LQG problem if we consider augmented system of the original system and previewed road inputs. The resulting optimal controller takes the form of augmented state feedback and the optimal estimator is given in the form of Kalman-Bucy filter involving the augmented states. Therefore, the separation theorem of wheelbase preview regulator problem is indirectly proved.

The contents of the paper will be organized as follows: In the next section, we will formulate active suspension design of a half car into a

discrete time, stochastic optimal, output feedback, wheelbase preview regulator problem. In Sec. 3, an augmented state vector is introduced to transform the problem into well-known LQG problem and then its optimal solution is derived. Numerical examples are given to verify performance of the resulting suspension in Sec. 4. And finally in Sec. 5, conclusions are drawn.

2. Problem Formulation

2.1 System model

Consider a half car model shown in Fig. 1.We assume that the rear tire travels over the same path as the front tire except for a time delay; hence $z_{0r}(t)=z_{0f}(t-\tau)$ where $\tau=\frac{a+b}{V}$. Assuming that the characteristics of all passive suspension elements are linear and that the pitch motion, θ, is small, the model can be described by the following equations:

$$\begin{aligned} M\ddot{z}_c &= f_f + f_r \\ I\ddot{\theta} &= f_f a - f_r b \\ m_f\ddot{z}_f &= -k_{f2}(z_f - z_{0f}) - f_f \\ m_r\ddot{z}_r &= -k_{r2}(z_r - z_{0r}) - f_r \end{aligned} \tag{1}$$

where f_f and f_r denote an upward front and rear suspension force, respectively, which are given by

$$\begin{aligned} f_f &= k_{f1}(z_f - z_c - a\theta) + b_f(\dot{z}_f - \dot{z}_c - a\dot{\theta}) + u_f \\ f_r &= k_{r1}(z_r - z_c + b\theta) + b_r(\dot{z}_r - \dot{z}_c + b\dot{\theta}) + u_r \end{aligned} \tag{2}$$

Relative displacements of the front and the rear suspension and accelerations of the sprung mass and the unsprung masses are assumed to be measured by relative displacement sensors and accelerometers under the noisy environments as follows:

$$y_1 = z_c + a\theta - z_f + \varepsilon_1 \quad y_2 = z_c - b\theta - z_r + \varepsilon_2$$

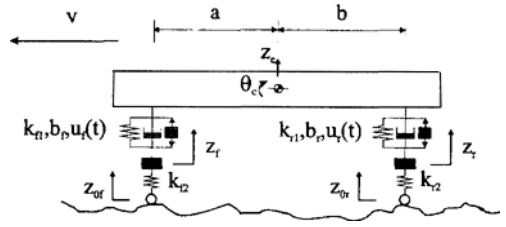

Fig. 1 A half car model.

$$\begin{aligned} y_3 &= \ddot{z}_c + \varepsilon_3 & y_4 &= \ddot{\theta} + \varepsilon_4 \\ y_5 &= \ddot{z}_f + \varepsilon_5 & y_6 &= \ddot{z}_r + \varepsilon_6 \end{aligned} \tag{3}$$

It is assumed that the measurement noises ε_is $(i=1, \cdots, 6)$ are white noise processes.

When we introduce the following state, control input, road input and measurement noise vectors,

$$\begin{aligned} x(t) &= [x_1, x_2, \cdots, x_8]^T \\ u(t) &= [u_f \;\; u_f]^T \\ w(t) &= [w_f \;\; w_r]^T \\ \varepsilon(t) &= [\varepsilon_1 \;\; \varepsilon_2 \;\; \varepsilon_3 \;\; \varepsilon_4 \;\; \varepsilon_5 \;\; \varepsilon_6]^T \end{aligned} \tag{4}$$

where

$$\begin{aligned} x_1 &= z_c + a\theta, & x_2 &= z_c - b\theta, \\ x_3 &= z_f, & x_4 &= z_r, \\ x_5 &= \dot{z}_c + a\dot{\theta}, & x_6 &= \dot{z}_c - b\dot{\theta}, \\ x_7 &= \dot{z}_f, & x_8 &= \dot{z}_r, \\ w_f(t) &= z_{0f}(t), & w_r(t) &= w_f(t-\tau), \end{aligned}$$

(1) and (3) can be expressed in terms of vector forms as follows:

$$\dot{x} = Ax + Bu + Ew \tag{5}$$

$$y = Cx + Du + Lw + \varepsilon \tag{6}$$

where A, B, E, C, D and L are given in Appendix A. Road profile is often approximated as a stationary stochastic process with the following auto-spectral density function:

$$S_{\text{road}}(\omega) = \frac{\sigma^2}{\pi} \cdot \frac{a_r v}{\omega^2 + (a_r v)^2} \tag{7}$$

where a_r and σ are constants depending on the type of road profile. (Kwak, 1993) Based on this function, the road input $w(t)$ can be modeled as a filtered white noise defined as follows:

$$\dot{w} = A_w w + B_w \psi \tag{8}$$

where

$$\begin{aligned} & A_w = -a_r v \begin{bmatrix} 1 & 0 \\ 0 & 1 \end{bmatrix}, \quad B_w = a_r \; v \begin{bmatrix} 1 & 0 \\ 0 & 1 \end{bmatrix}, \\ & \psi(t) = [\psi_f(t) \;\; \psi_r(t)]^T, \\ & E[\psi(t)] = 0, \\ & \operatorname{cov}[\psi(t)] = \tilde{\Psi}(t) = 2\sigma^2 \begin{bmatrix} 1 & 0 \\ 0 & 1 \end{bmatrix} \geq 0, \\ & E[\psi_f(t)\psi_r^T(\tau)] = 2\sigma^2\delta(t - \tau + \tau) \begin{bmatrix} 1 & 0 \\ 0 & 1 \end{bmatrix} \end{aligned} \tag{9}$$

Note that the relation between w_f and w_r, $w_r(t) = w_f(t-\tau)$ is now expressed by the correlation

between ϕ_f and ϕ_r. We assume that the initial condition $x(0)$ and measurement noise $\varepsilon(t)$ satisfy the following conditions:

$$E[x(0)]=\bar{x}(0),\quad \mathrm{cov}[x(0)]=\tilde{P}(0)\geq 0,$$
$$E[\varepsilon(t)]=0,\quad \mathrm{cov}(\varepsilon(t)]=\tilde{E}(t)>0,$$
$$E[\phi(t)\varepsilon^T(\tau)]=0 \tag{10}$$

2.2 Performance index

The purpose of the active suspension is assumed to reduce the required suspension working space and the maximum acceleration of the sprung mass, without increasing the dynamic tire force variation too severely. Finally, for practical reasons, the magnitude of control force is limited. These objectives can be achieved by finding the optimal input that minimizes the following performance index:

$$J=\frac{1}{2}E\left[\int_0^{T_f}\left\{\begin{bmatrix}\dot{z}_c\\ \ddot{\theta}\end{bmatrix}^T\begin{bmatrix}\rho_1 & 0\\ 0 & \rho_2\end{bmatrix}\begin{bmatrix}\dot{z}_c\\ \ddot{\theta}\end{bmatrix}+\begin{bmatrix}x_1-x_3\\ x_2-x_4\end{bmatrix}^T\right.\right.$$
$$\left.\left.\begin{bmatrix}\rho_3 & 0\\ 0 & \rho_4\end{bmatrix}\begin{bmatrix}x_1-x_3\\ x_2-x_4\end{bmatrix}+\begin{bmatrix}x_3-w_f\\ x_4-w_r\end{bmatrix}^T\begin{bmatrix}\rho_5 & 0\\ 0 & \rho_6\end{bmatrix}\right\}dt$$
$$\left.+\begin{bmatrix}x_3-w_f\\ x_4-w_r\end{bmatrix}+\begin{bmatrix}u_f\\ u_r\end{bmatrix}^T\begin{bmatrix}\rho_7 & 0\\ 0 & \rho_8\end{bmatrix}\begin{bmatrix}u_f\\ u_r\end{bmatrix}\right] \tag{11}$$

where $\rho_i(1\leq i\leq 8)$ is a weighting constant determined by designers. By expressing the sprung mass acceleration and the suspension deflection in terms of state, control input and road input vectors, the performance index can be written as the following quadratic form:

$$J=\frac{1}{2}E\left[\int_0^{T_f}\{x^TQ_1x+2x^TNu+u^T\tilde{R}u+2x^TQ_{12}w\right.$$
$$\left.+w^TQ_2w\}dt+x^T(T_f)S_1x(T_f)+2x^T(T_f)S_{12}w(T_f)S_2w(T_f)\right] \tag{12}$$

where

$$\begin{bmatrix}Q_1\\ Q_{12}^T\end{bmatrix}\geq 0,$$
$$\begin{bmatrix}S_1 & S_{12}\\ S_{12}^T & S_2\end{bmatrix}=0,$$
$$\begin{bmatrix}Q_1 & Q_{12}\\ Q_{12} & Q_2\end{bmatrix}-\begin{bmatrix}N^T\\ 0\end{bmatrix}\tilde{R}^{-1}[N^T\ \ 0]\geq 0,\ \tilde{R}>0.$$

2.3 Discretization

With a sampling time T_s, discrete-time representation of (5), (6) and (8) takes the following form:

$$x(k+1)=Gx(k)+Hu(k)+Fw(k) \tag{13}$$
$$w(k+1)=G_ww(k)+\phi'(k) \tag{14}$$
$$y(k)=Cx(k)+Du(k)+Lw(k)+\varepsilon(k) \tag{15}$$

where G, H, F, G_w and $\phi'(k)$ are discrete equivalents of A, B, E, A_w and $B_w\phi(t)$, respectively. Discrete equivalents of statistical conditions in (9) and (10) are given as

$$E[x(0)]=\bar{x}(0),$$
$$\mathrm{cov}[\phi'(k)]=\Psi'(k)\geq 0$$
$$\mathrm{cov}[x(0)]=P(0)\geq 0,$$
$$\mathrm{cov}[\varepsilon(k)]=E(k)>0 \tag{16}$$

and in discrete-time domain the correlation between front and rear disturbances is expressed as

$$E[\phi_f'(k)\{\phi_r'(\tilde{k})\}^T]=\Psi_f'(k)\delta(k-\tilde{k}+N_\tau) \tag{17}$$

where $N_\tau=\frac{\tau}{T_s}$. Finally, the performance index, (12) can be transformed into the following discrete equivalent by using the discretization method given in (Franklin, 1990).

$$J=\frac{1}{2}E\left[\begin{pmatrix}x(n)\\ w(n)\end{pmatrix}^T\begin{bmatrix}S_{xx}(n) & S_{xw}(n)\\ S_{xw}(n) & S_{ww}(n)\end{bmatrix}\begin{pmatrix}x(n)\\ w(n)\end{pmatrix}\right.$$
$$+\sum_{n=0}^{\infty}\left\{\begin{pmatrix}x(i)\\ wi\end{pmatrix}^T\begin{bmatrix}Q_{xx} & Q_{xw}\\ Q_{xw} & Q_{ww}\end{bmatrix}\begin{pmatrix}x(i)\\ w(i)\end{pmatrix}\right.$$
$$\left.\left.+2\begin{pmatrix}x(i)\\ w(i)\end{pmatrix}^T\begin{bmatrix}M_x\\ M_w\end{bmatrix}u(i)+u^T(i)Ru(i)\right\}\right] \tag{18}$$

where

$$Q=\begin{bmatrix}Q_{xx} & Q_{xw}\\ Q_{xw} & Q_{ww}\end{bmatrix}\geq 0,$$
$$S=\begin{bmatrix}S_{xx}(n) & S_{xw}(n)\\ S_{xw}(n) & S_{xw}(n)\end{bmatrix}=0,$$
$$Q-\begin{bmatrix}M_x\\ M_w\end{bmatrix}R^{-1}[M_x^T\ \ M_w^T]\geq 0,\ R>0,$$
$$n=\frac{T_f}{T_s}.$$

3. Stochastic Optimai Observer-Based Wheelbase Preview Regulator Problem

Consider the following augmented state vector

$$x_a(k)=\begin{bmatrix} x(k) \\ w_f(k-N_\tau) \\ \vdots \\ w_f(k) \end{bmatrix} \tag{19}$$

Noting that $w_r(k)=w_f(k-N_\tau)$, its state equations can be written as

$$x_a(k+1)=G_a x_a(k)+H_a u(k)+\phi_a(k) \tag{20}$$

where

$$G_a=\begin{bmatrix} G & F_r & 0 & \cdots & F_f \\ 0 & 0 & I & & 0 \\ & & & & \\ & & & & I \\ 0 & 0 & 0 & \cdots & G_f \end{bmatrix},$$

$$H_a=\begin{bmatrix} H \\ 0 \\ \vdots \\ 0 \\ 0 \end{bmatrix},\quad \phi_a(k)=\begin{pmatrix} 0 \\ 0 \\ \vdots \\ 0 \\ \phi_f'(k) \end{pmatrix},$$

$$F=[F_f \;\; F_r],\quad \phi'(k)=[\phi_f'(k) \;\; \phi_r'(k)],$$

$$G_w=\begin{bmatrix} G_f & 0 \\ 0 & G_r \end{bmatrix} \tag{21}$$

And (15) can be expressed in terms of the augmented vector as,

$$y(k)=C_a x_a(k)+Du(k)+\varepsilon(k) \tag{22}$$

$$C_a=[C \;\; L_r \; 0 \cdots L_f],\quad L=[L_f \;\; L_r] \tag{23}$$

The initial condition, $x_a(0)$ and the system noise vector, ϕ_a of the augmented system satisfy the following conditions:

$$E[x_a(0)]=[\bar{x}(0)^T \; 0 \cdots 0]^T$$

$$\mathrm{cov}[x_a(0)]=P_a(0)=\begin{bmatrix} P(0) & 0 & \cdots & 0 \\ 0 & 0 & \cdots & 0 \\ \vdots & \vdots & & \vdots \\ 0 & 0 & \cdots & 0 \end{bmatrix}\geq 0$$

$$\mathrm{cov}[\phi_a(k)]=\Psi_a(k)=\begin{bmatrix} 0 & 0 & 0 & \cdots & 0 \\ 0 & 0 & 0 & \cdots & 0 \\ & & & & \vdots \\ & & & 0 & 0 \\ 0 & 0 & 0 & \cdots & \Psi_f'(k) \end{bmatrix}\geq 0 \tag{24}$$

where $\Psi'(k)=\begin{bmatrix} \Psi_f'(k) & 0 \\ 0 & \Psi_r'(k) \end{bmatrix}$. The performance index in (18) is expressed in terms of the augmented state vector as

$$J=\frac{1}{2}E\begin{bmatrix} x_a^T(n)\,S_a(n)\,x_a(n)+\sum_{n=0}^{\infty}\{x_a^T(i)\,Q_a x_a \\ (i) \\ +2x_a^T(i)\,M_a u(i)+u^T(i)\,Ru(i)\} \end{bmatrix} \tag{25}$$

where

$$Q_a=\begin{bmatrix} Q_{xx} & Q_{xr} & 0 & \cdots & Q_{xf} \\ & Q_{rr} & 0 & \cdots & Q_{rf} \\ & \text{symmetric} & 0 & \cdots & 0 \\ & & & & \vdots \\ & & & & Q_{ff} \end{bmatrix}\geq 0,$$

$$S_a(n)=\begin{bmatrix} S_{xx} & S_{xr} & 0 & \cdots & S_{xf} \\ & S_{rr} & 0 & \cdots & S_{rf} \\ & & 0 & \cdots & 0 \\ & \text{symmetric} & & & \vdots \\ & & & & S_{ff} \end{bmatrix}\geq 0,$$

$$M_a=\begin{bmatrix} M_x \\ M_r \\ 0 \\ \vdots \\ M_f \end{bmatrix},\quad S_{xw}(n)=[S_{xf}(n) \;\; S_{xr}(n)]=0,$$

$$S_{ww}(n)=\begin{bmatrix} S_{ff}(n) & S_{rf}^T(n) \\ S_{rf}(n) & S_{rr}(n) \end{bmatrix}=0,$$

$$Q_{xw}=[Q_{xf} \;\; Q_{xr}],\quad Q_{ww}=\begin{bmatrix} Q_{ff} & Q_{rf}^T \\ Q_{rf} & Q_{rr} \end{bmatrix},$$

$$M_a=\begin{bmatrix} M_f \\ M_r \end{bmatrix},\quad Q_a-M_a R^{-1}M_a^S\geq 0 \tag{26}$$

We note that by using the augmented state vector, the stochastic optimal observer-based wheelbase preview regulator problem reduces to a classical LQG problem. It may be easily proved that the separation theorem holds for the LQG problem and that its solution is the combination of a deterministic optimal state feedback control and a stochastic optimal estimator. The optimal solution to the LQG problem is reproduced in the following theorem. (Åström, 1970)

Theorem 1.

The optimal solution of the LQG problem is the same as the solution to the linear quadratic regulator (LQR) problem except that in the control law the state $x_a(k)$ is replaced with its estimate $\hat{x}_a(k)$. The optimal input, $u^*(k)$ $(k\geq 0)$ is given by

$$u^*(k)=-K_c(k)\hat{x}_a(k), \tag{27}$$

where $K_c(k)$ is the gain matrix for the optimal regulator such as

$$K_c(k)=\left[R+H_a{}^TP_c(k+1)H_a\right]^{-1}(H_a{}^TP_c(k+1)G_a+M_a{}^T) \tag{28}$$

and matrix $P_c(k)$ satisfies the discrete Riccati equation

$$P_c(k)=\hat{G}_a{}^TP_c(k+1)\hat{G}_a+\hat{Q}_a-\hat{G}_a{}^TP_c(k+1)H_a[R+H_a{}^TP_c(k+1)H_a]^{-1}H_a{}^TP_c(k+1)\hat{G}_a \tag{29}$$

with initial condition $P_c(n)=S_a(n)$ and,

$$\hat{G}_a=G_a-H_aR^{-1}M_a{}^T$$
$$\hat{Q}_a=Q_a-M_aR^{-1}M_a{}^T \tag{30}$$

$\hat{x}_a(k)$ is the conditional mean of $x_a(k)$ given $y_a(j)$, $0\le j\le k$; $\hat{x}_a(k)$ can be obtained as the output of the optimal estimator described as

$$\hat{x}_a(k+1)=G_a\hat{x}_a(k)+H_au(k)+K_e(k)[y(k)-\hat{y}(k)],\ \hat{y}(k)=C_a\hat{x}_a(k)+Du(k) \tag{31}$$

The optimal estimator gain $K_e(k)$

$$K_e(k)=G_aP_e(k)C_k{}^T[C_aP_e(k)C_a{}^T+E(k)]^{-1} \tag{32}$$

is obtained from the discrete Riccati equation,

$$P_e(k+1)=G_aP_e(k)G_a{}^T+\Psi_a(k)-G_aP_e(k)C_a{}^T[C_aP_e(k)C_a{}^T+E(k)]^{-1}C_aP_e(k)G_a{}^T \tag{33}$$

with initial condition $P_e(0)=P_a(0)$.

The minimal performance index achievable with the optimal control input (27) is given as

$$\min_u E[J]=\frac{1}{2}\left[\begin{array}{l}\bar{x}_a(0)^TP_c(0)\bar{x}_a(0)+\mathrm{tr}[P_c(0)P_e(0)]\\+\sum_{i=0}^{n-1}\mathrm{tr}[P_c(i+1)\Psi_a]+\sum_{i=0}^{n-1}\mathrm{tr}[P_e(i)K_c{}^T(i)\\[H_a{}^TP_c(i+1)H_a+R]K_c(i)]\end{array}\right] \tag{34}$$

We note that orders of resulting controller and estimator are much larger than that of the original system. Furthermore, their orders, $n+N_\tau+1$, change with a vehicle speed, which means that the controller should be modified as the vehicle speed changes. For implementation of the proposed controller in real applications, methods of reducing its computational burden should be further investigated, which is left for a future study.

4. Numerical Examples

In this section, the results of the previous section are applied to the vehicle suspension system described in Sec. 2.The parameter values used in the simulation are given as

$$\begin{array}{ll}M=500\text{kg}, & I=910\ \text{kg}\cdot\text{m}^2\\ m_f=30\text{kg} & m_r=40\ \text{kg}\\ a=1.25\ \text{m}, & b=1.45\ \text{m},\\ k_{f1}=1000\ \text{N/m}, & k_{r1}=10000\ \text{N/m},\\ k_{f2}=100000\ \text{N/m}, & k_{r2}=100000\ \text{N/m},\\ b_f=1000\ \text{N}\cdot\text{sec/m}, & b_r=1000\ \text{N}\cdot\text{sec/m}.\end{array} \tag{35}$$

They correspond to a compact sedan. (Hac, 1993) We used the following values for the road model, which represents characteristics of a paved road. (Kwak, 1993)

$$a_r=0.45\ 1/\text{m},\ \sigma^2=300\times10^{-6}\text{m}^2 \tag{36}$$

A vehicle is assumed to run straight ahead with a constant speed and the sampling time, T_s is set to 0.01 sec, considering that all the modal frequencies of the system is less than 10 Hz.

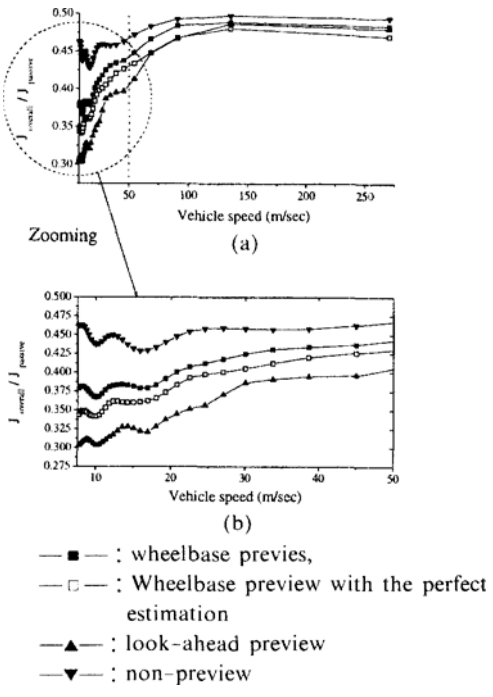

Fig. 2 Comparison of overall performances for a given range of speeds.

For the performance index defined in (11), we used the following weightings:

$$\rho_1 = 7.938e-1, \quad \rho_2 = 1.236e+0,$$
$$\rho_3 = 3.555e+2, \quad \rho_4 = 6.274e+2,$$
$$\rho_5 = 1.191e+1, \quad \rho_6 = 1.270e+2,$$
$$\rho_7 = 2.000e-8, \quad \rho_8 = 2.000e-8. \tag{37}$$

It corresponds to the controller whose main objective is to improve the ride comfort. As for measurement variables, we assume that heave and pitch accelerations of the sprung mass, suspension deflections and accelerations of the unsprung masses are available. Covariance matrices of measurement noises are selected as

$$\tilde{E}(t) = \text{diag}(9.856e-8,\ 5.609e-8,\ 4.440e-4,\ 2.856e-4,\ 2.533e-1,\ 1.559e-1), \tag{38}$$

to make signal to noise ratios equal to 15dB. Based on the parameters given above, a stochastic optimal observer-based wheelbase preview regulator was designed.

In Fig. 2, overall performances of wheelbase preview, look-ahead preview and non-preview control systems are compared for the speeds ranging from 7.5 m/sec (=27 km/h) to 275 m/sec (=990 km/h). The look-ahead preview control system was assumed to measures the future road inputs so that the front suspension can have the preview information corresponding to wheelbase preview distance, $a+b$. As a vehicle speed changes in a given range, preview step decreases from 367 to 1 and accordingly the amount of preview information available for control diminishes. Optimal performance index of the preview control system is expected to monotonically increase with the speed. All the performance indices in the figures are normalized by that of the passive system. In Fig. 2(a), the performance of wheelbase preview control system is better than that of the non-preview control system but worse than that of the look-ahead preview control system. The differences in their performances result from the differences in the preview information that are available for control scheme. As expected, the differences decrease as the vehicle speed goes high. In Fig. 2(b), Figure 2(a) is magnified for the speed range of 7.5 m/sec (=27 km/h) ~50 m/sec (=180 km/h) which can be said to be a normal operating range of automobiles. For 7.5 m/sec, the wheelbase preview and the look-ahead preview system have the performance improvement of 18%, 35%, respectively, over the passive system, while they have improvement of 13%, 5.4% for 50 m/sec, respectively. We can conclude that, in this example, the look-ahead preview control system has the performance two times better than the wheelbase preview control system.

To investigate performance degradation by estimation errors, performance of the wheelbase preview control system is compared with that of the wheelbase preview control system with the perfect estimation. In Fig. 2(b), the performance of the wheelbase preview control system deteriorates from that of the wheelbase preview system with the perfect estimation. The performance deterioration by estimation errors decreases as the vehicle speed increases. It is due to the fact that for measurement noises having the constant covariance in (38), the S/N ratios of measurements improve with increase of the vehicle speed.

In Fig. 2(a), we note that the performance index of the preview control system does not converge to that of the non-preview controller even if the vehicle speed becomes very high. It can be attributed to the fact that in addition to absence of preview information, performance of the non-preview control system is deteriorated by the estimation errors that result from neglecting the correlation between front and rear road inputs. In Fig. 3(a) and (b), the control and estimation performance indices of the wheelbase preview and non-preview control systems are shown, respectively. The control performance index accounts for control performance when estimation error is assumed to be zero and the estimation performance index accounts for performance deterioration by estimation errors. In Fig. 3(a), control performance indices of two control systems become almost same when a vehicle speed is high enough. But as for estimation performance in Fig. 3(b), their difference does not decrease with the speed but keeps a constant value. This explains why preview control system shows better performance than that of non-preview control system even when vehicle speed becomes so high

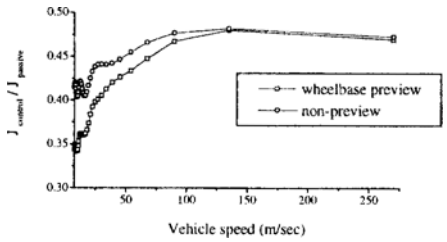

(a) Control performances under perfect estimation

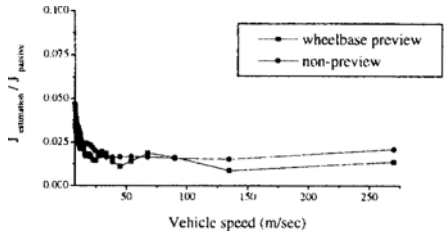

(b) Performance degradation by estimation errors

Fig. 3 Comparison of control and estimation performances of wheelbase preview and non-preview control systems.

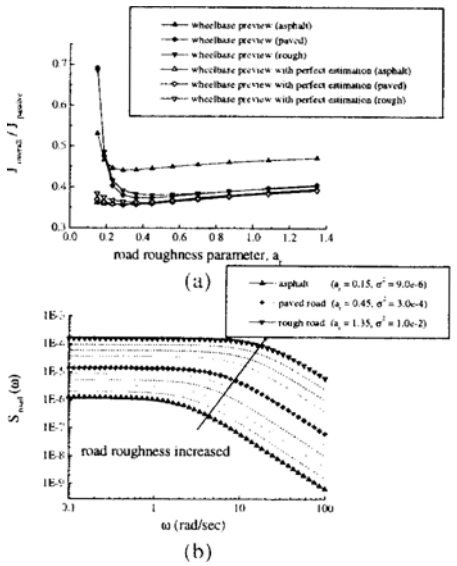

Fig. 4 Performance degradation caused by road model errors.

that wheelbase preview information is not available.

Now, we examine how the wheelbase preview control works when road model errors exist. In Fig. 4 (b), auto spectral density functions of several road models are shown. Among these models, we selected three road models that represent characteristics of asphalt road, paved road and rough road and we designed optimal wheelbase preview control system based on the selected models. The changes of performance indices of these controllers with road model errors are shown in Fig. 4 (a). Again, performance indices of the wheelbase preview control system with perfect estimation that are based on the same models are also shown. From the figure, the performances of the preview control systems are more sensitive to road model errors than those of the preview control systems with perfect estimation. We can conclude that for implementation of preview control in real applications, we need to determine online on which road condition a vehicle is running and tune the control parameters accordingly.

5. Conclusions

In this paper, we derived the solution of the stochastic optimal observer-based wheelbase preview regulator problem. It has been proven that the separation theorem holds and a controller and an estimator can be designed without reference to each other as in the classical linear quadratic Gaussian problem. The resulting optimal control input is in the form of feedback input involving the augmented state that is estimated by Kalman-Bucy filter. The optimal solution requires the solution of Riccati equations whose dimensions are much larger than the original system order at each step and thus methods of reducing computational burden remain as a future study. By the numerical simulation of a half car model, we showed that performance improvement of wheelbase preview control system over the non-preview system amounts to half of the performance improvement possible with look-ahead preview system. It was also shown that due to estimation errors, the performance of wheelbase preview control is sensitive to road model errors. It was suggested that, for practical implementation of wheelbase preview control, the online modeling of road profiles and the subsequent online tuning of control parameter would be necessary.

References

Antonio, M. and Masao, Nagai, 1992, "Optimal Preview Control of Rear Suspension Using Nonlinear Neural Networks," *Proceeding of the International Symposium on Advanced Vehicle Control,* pp. 117~122.

Araki Y., Oya M., and Harada H., 1994, "Preview Control of Active Suspension Using Disturbance of Front Wheel," *Proceeding of the International Symposium on Advanced Vehicle Control,* pp. 299~304.

Åström, K. J., 1970, Linear Stochastic Control Theory, "Introduction to Stochastic Control Theory," Academic Press, SAN DIEGO, pp. 256~294.

Bender, E. K., 1968, "Optimum Linear Preview Control with Application to Vehicle Suspension," *ASME Journal of Basic Engineering,* Ser. D, Vol. 90, No. 2, pp. 213~221.

Crolla D. A. and Abdel-Hady M. B. A., 1991, "Active Suspension Control; Performance Comparisons Using Control Laws Applied to a Full Vehicle Model," *Vehicle System Dynamics,* Vol. 20, pp. 107~120.

Franklin, G. F., Powell, J. D. and Workman, M. L., 1990, "Multivariable and Optimal Control," *Digital Control of Dynamic Systems, 2nd Edition, Addison Wesley,* pp. 417~482.

Hac, A. and Youn, I., 1993, "Optimal Design of Active and Semi-Active Suspensions Including Time Delays and Preview," *ASME Journal of Vibration and Acoustics,* Vol. 115, pp. 498~508.

Huisman, R. G. M., Veldpaus, F. E., van Heck, J. G. A. M. and Kok, J. J., 1994, "Application of a Preview Controlled Active Suspension to a (Non)linear 2-D Truck Model," *Proceeding of the International Symposium on Advanced Vehicle Control,* pp. 293~298.

Jang, J. -H., and Han, C. -S., 1997, "Sensitivity Analysis of Side Slip Angle for a Front Wheel Steering Vehicle: A Frequency Domain Approach," *KSME International Journal,* Vol. 11, No. 4, pp. 367~378.

Kwak, B. -H., 1993, "*A Study on the Robust Active Suspension Controller Design,*" Master Thesis, Korea Advanced Institute of Science and Technology, Dept. Of Mechanical Engineering.

Louam, N., Wilson, D. A. and Sharp, R. S., 1988, "Optimal Control of a Vehicle Suspension Incorporating the Time Delay Between Front and Rear Wheel Inputs," *Vehicle System Dynamics,* Vol. 17, pp. 317~336.

Pilbeam, C. and Sharp, R. S., 1993, "On the Preview Control of Limited Bandwidth Vehicle Suspensions," Proc of Instn Mech Engrs, Part D: *Journal of Automobile Engineering,* Vol. 207, pp. 185~193.

Roh, H. -S. and Park, Y., 1997, "Stochastic Optimal Preview Control of Active Suspension," Vehicle System Dynamics, (submitted).

Yong, B., 1997, "Contour-Following of a Force-Controlled Industrial Robot Using Preview Control," *KSME International* Journal, Vol. 11, No. 2, pp. 115~124.

Appendix

A. Definition of A, B, C, D, E and L.

$$A=\begin{bmatrix} 0 & I \\ A_{21} & A_{22} \end{bmatrix},\quad B=\begin{bmatrix} 0 \\ B' \end{bmatrix},$$

$$C=\begin{bmatrix} 1 & 0 & -1 & 0 & 0 & 0 & 0 & 0 \\ 0 & 1 & 0 & -1 & 0 & 0 & 0 & 0 \\ -\frac{k_{f1}}{M} & -\frac{k_{r1}}{M} & \frac{k_{f1}}{M} & \frac{k_{r1}}{M} & -\frac{b_f}{M} & -\frac{b_r}{M} & \frac{b_f}{M} & \frac{b_r}{M} \\ -a\frac{k_{f1}}{I} & b\frac{k_{r1}}{I} & a\frac{k_{r1}}{I} & -b\frac{k_{r1}}{I} & -a\frac{B_f}{I} & b\frac{b_r}{I} & a\frac{b_f}{I} & -b\frac{b_r}{I} \\ \frac{k_{f1}}{m_f} & 0 & -\frac{k_{f2}}{m_f} & 0 & \frac{b_f}{m_f} & 0 & -\frac{b_f}{m_f} & 0 \\ 0 & \frac{k_{r1}}{m_r} & 0 & -\frac{k_{r2}}{m_r} & 0 & \frac{b_r}{m_r} & 0 & -\frac{b_r}{m_r} \end{bmatrix}$$

$$D=\begin{bmatrix} 0 & 0 \\ 0 & 0 \\ \frac{1}{M} & \frac{1}{M} \\ \frac{a}{I} & -\frac{b}{I} \\ -\frac{1}{m_f} & 0 \\ 0 & -\frac{1}{m} \end{bmatrix},\quad E=\begin{bmatrix} 0 \\ E' \end{bmatrix},\quad L=\begin{bmatrix} 0 & 0 \\ 0 & 0 \\ 0 & 0 \\ 0 & 0 \\ \frac{k_{f2}}{m_f} & 0 \\ 0 & \frac{k_{r2}}{m_r} \end{bmatrix}$$

where

$$A_{21}=\begin{bmatrix} -a_1k_{f1} & -a_2k_{r1} & a_1k_{f1} & a_2k_{r1} \\ -a_2k_{f1} & -a_3k_{r1} & a_2k_{f1} & k_3k_{r1} \\ \dfrac{k_{f1}}{m_f} & -\dfrac{k_{f1}+k_{f2}}{m} & 0 & 0 \\ \dfrac{k_{r1}}{m_r} & -\dfrac{k_{r1}+k_{r2}}{m_r} & 0 & 0 \end{bmatrix},$$

$$A_{22}=\begin{bmatrix} -a_1b_f & -a_2b_r & a_1b_f & a_2b_r \\ -a_2b_f & -a_3b_r & a_2b_f & a_3b_r \\ 0 & 0 & -\dfrac{b_f}{m_f} & 0 \\ 0 & 0 & 0 & -\dfrac{b_r}{m_r} \end{bmatrix},$$

$$B'=\begin{bmatrix} a_1 & a_2 \\ a_2 & a_3 \\ -\dfrac{1}{m_f} & 0 \\ 0 & -\dfrac{1}{m_r} \end{bmatrix},\quad E'=\begin{bmatrix} 0 & 0 \\ 0 & 0 \\ \dfrac{k_{f2}}{m_f} & 0 \\ 0 & \dfrac{k_{r2}}{m_r} \end{bmatrix},$$

$$a_1=\frac{1}{M}+\frac{a^2}{I},\quad a_2=\frac{1}{m}-\frac{ab}{I},\quad a_3=\frac{1}{M}+\frac{b^2}{I}.$$